

---

# **SHAMRC Environment and Vehicle Loads Calculations for Non-Ideal Flow**

**by  
Joseph Crepeau, Charles Needham and Robert Newell**

Prepared for:

The High Performance Computing Modernization Program (HPCMP)  
2002 Users Group Conference

Austin, TX  
June 10-13, 2002

## **Applied Research Associates, Inc.**

4300 San Mateo Blvd. NE, Suite A-220  
Albuquerque, New Mexico 87110  
(505) 883-3636

---

## Table of Contents

Introduction.....	1
The Code.....	1
Calculational Models .....	3
Dust Injection Model .....	5
HPC Resources Used .....	6
Data Comparisons .....	6
Summary .....	12
References.....	13

---

## List of Figures

Figure 1 Scalability of 2D SHAMRC for a variable-size problem. Comparison of the calculated versus ideal whiz factor for up to 64 processors.....	3
Figure 2 SHAMRC calculational model for the environment characterization simulations....	4
Figure 3 SHAMRC calculational model of M-110A2 for the vehicle loads simulation. ....	5
Figure 4 Waveform comparison between environment characterization test and SHAMRC. SHAMRC Calculations with (green, dashed) and without (red, dotted) dust. The insert shows the location of this station in yellow.....	8
Figure 5 Overpressure waveform comparison between experimental gage recording (black) and SHAMRC calculation (blue) on upstream side of vehicle. The insert shows the stations on the vehicle surface (blue dots) and the location of this station in red.....	9
Figure 6 Overpressure waveform comparison between experimental gage recording (black) and SHAMRC calculation (blue) on bottom of vehicle. The insert shows the stations on the vehicle surface (blue dots) and the location of this station in red.....	10
Figure 7 Overpressure waveform comparison between experimental gage recording (black) and SHAMRC calculation (blue) on downstream side of vehicle. The insert shows the stations on the vehicle surface (blue dots) and the location of this station in red.....	11
Figure 8 Comparison of test video with SHAMRC image at 690 ms. ....	11

## Introduction

High Performance Computing (HPC) resources have enabled scientists and engineers at Applied Research Associates (ARA), Inc. to perform high fidelity computational fluid dynamics (CFD) calculations in support of the Defense Threat Reduction Agency (DTRA) Non-Ideal Air Blast (NIAB) program. The NIAB program seeks to quantify the effects of NIAB on military vehicles over a wide range of geographical areas and scenarios. Of particular interest is the ability to simulate computationally the environment and vehicle loads from the exit jet produced by the DTRA Large Blast and Thermal Simulator (LB/TS) located at White Sands, New Mexico. The calculations were run with the parallel version of SHAMRC (Second-order Hydrodynamic Automatic Mesh Refinement Code) (Reference 1) and leveraged the HPC resources to produce timely and accurate results.

This paper presents the results of three-dimensional (3D) SHAMRC calculations of the airblast environments and loads on a military vehicle from the exit jet of the LB/TS. It presents the code and the computational models used. Comparisons with experimental gage recordings and high-speed photographic data are also presented. The results of the SHAMRC simulations are in excellent agreement with the experimental data. A more detailed writeup of the results is presented in Reference 2.

The results of the simulations demonstrate the viability of using SHAMRC to help predict equipment damage from nuclear blast effects. Without the use of HPC facilities these calculations could not have been completed within the given time constraints. The rapid turn around time allowed us to provide DTRA with timely, accurate results.

## The Code

SHAMRC (pronounced shamrock) is a two- and three-dimensional, finite difference, hydrodynamic computer code. SHAMRC is a descendant of SHARC (Second-order Hydrodynamic Advanced Research Code). It is used to solve a variety of airblast related problems which include high explosive (HE) detonations, nuclear explosive (NE) detonations, structure loading, thermal effects on airblast, cloud rise, conventional munitions blast and fragmentation, shock tube phenomenology, dust and debris dispersion, and atmospheric shock propagation. The code has the capability to run with a single Eulerian grid or with the Automatic Mesh Refinement (AMR) option that divides the calculational domain into smaller Eulerian grids at several levels of refinement to provide high-resolution results.

Its capabilities and attributes include multiple geometries, non-responsive structures, non-interactive and interactive particles, several atmosphere models, multi-materials, a large material library, HE detonations, a  $K-\epsilon$  turbulence model, and water and dust vaporization. SHAMRC is second-order accurate in both space and time and is fully conservative of mass, momentum and energy. It is fast because it employs a structured Eulerian grid and efficient due to the use of the pre-processor SRCLIB. SHAMRC is a production research code.

SHAMRC is a government-owned, non-proprietary CFD code under export controls that has been supported and developed by DTRA over the past 30 years. It currently has the capability to

run in single-grid mode or with an adaptive mesh refinement (AMR), both of which have been parallelized to take advantage of the rapidly developing hardware improvements, and ensure the viability of the code. The AMR capability of SHAMRC allows the efficient calculation of certain classes of problems that are otherwise intractable using the conventional single-grid method.

The programs and mission areas being supported by this code are many and varied. While not all applications of the code are monitored, some of the programs that have been supported by SHAMRC calculations within the last several years include:

1. Anti-Terrorism program test design, loads predictions and analysis
2. Force Protection program test design, loads predictions and analysis
3. Chemical/Biological source modeling for agent release, entrainment, and plume formation
4. Conventional weapons blast and fragment predictions, including weapon characterization test support and munitions design and evaluation
5. High explosive test design and analysis including shaped charges, and free field detonations
6. Hardened Underground Structures Program test design, predictions and analysis
7. RAM Jet/SCRAM jet flow and chemical reactions
8. Gaseous detonations and fuel air explosive blast definition and propagation
9. Nuclear ideal and non-ideal blast wave definition and prediction
10. Shock tube performance, blockage, boundary layer definition and effects, and transitory turbulent circular jets
11. Thermobaric ACTD

SHAMRC has been parallelized to run on large scalable parallel platforms. It uses the Message Passing Interface (MPI) library to achieve parallelism. Initial versions of the code were parallelized in 3D only and the Eulerian grid was decomposed in only one dimension. The calculations reported in this paper utilized this parallel model. Since that time, the code has been modified to perform automatic domain decomposition on the Eulerian grid in up to three dimensions for both the 2D and 3D versions of the code. The parallel version of SHAMRC has been tested on several parallel platforms.

SHAMRC exhibits good scalability. Figure 1 is a comparison of the “whiz factor”, the computational time per cell per cycle, from timing calculations with the ideal whiz factor, which assumes perfect scalability. The timing calculations were run on the Compaq ES40 at the Aeronautical Systems Center (ASC). The chosen test problem was scalable, where the number of zones per processor was fixed over a range of 2 to 64 processors. It is clear from the comparison that nearly ideal scalability was achieved for up to 64 processors. Unfortunately, processor availability prohibited us from determining the scalability above 64 processors. A similar study was attempted on the 3D code but was not completed. The scalability behavior of the 3D code is expected to be similar to that of the 2D code.

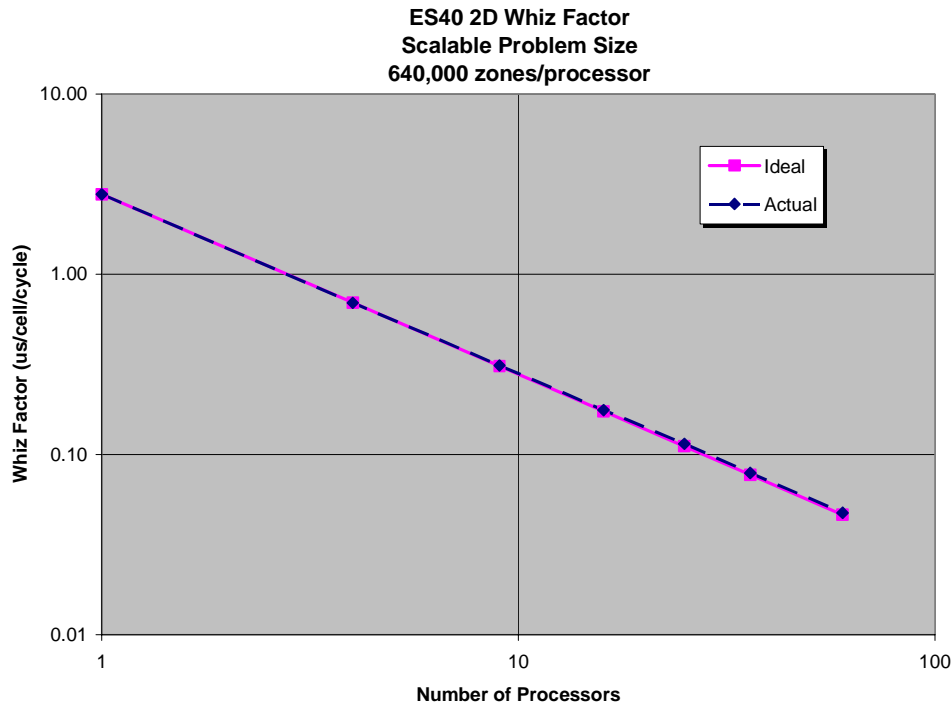


Figure 1 Scalability of 2D SHAMRC for a variable-size problem. Comparison of the calculated versus ideal whiz factor for up to 64 processors.

## Calculational Models

Three, 3D calculations were run. The first two calculations computed the exterior environment produced by the exit jet from the LB/TS, which is used to simulate non-ideal airblast produced from a nuclear weapon. Non-ideal airblast is characterized by high dynamic pressures and relatively low overpressures, with an extended positive duration of heavily dust-laden flow. Because the test section and access berms were constructed of sand, it was thought that the sand might modify the flow depending on the amount of sand (dust) that became entrained in the flow. The first environment calculation ignored the dust contribution. The second environment calculation included a dust injection model that is currently available in SHAMRC to simulate the effects of the dust scoured from the berm region.

All calculations modeled the last 25 meters of the shock tube and its interior and the structures and terrain exterior to the shock tube. The calculational grid for the environment calculations contained approximately 48 million zones. Over 5,000 monitoring points were placed in the calculation to record time-history data for comparison with experimental results. Figure 2 shows the calculational model used for the environment calculations. The blue dots represent the locations of “stations” placed in the calculational grid. Stations record time-histories for several field variables.

The third calculation modeled a test of the non-ideal blast effects on an M-110A2 self-propelled Howitzer. It included a non-responding model of the M-110A2 on a 3-cm resolution subgrid located 25 meters from the end of the shock tube and centered on the test berm. It also included

the same dust injection model used in one of the environment calculations. The calculational grid contained over 150 million zones. Stations were placed around and on the vehicle exterior at numerous locations, including those corresponding to experimental gages. The station recordings were used to provide input for vehicle response calculations. Figure 3 shows the vehicle as modeled in the loads calculation. The structures outside the LB/TS were the same as in the environments calculations.

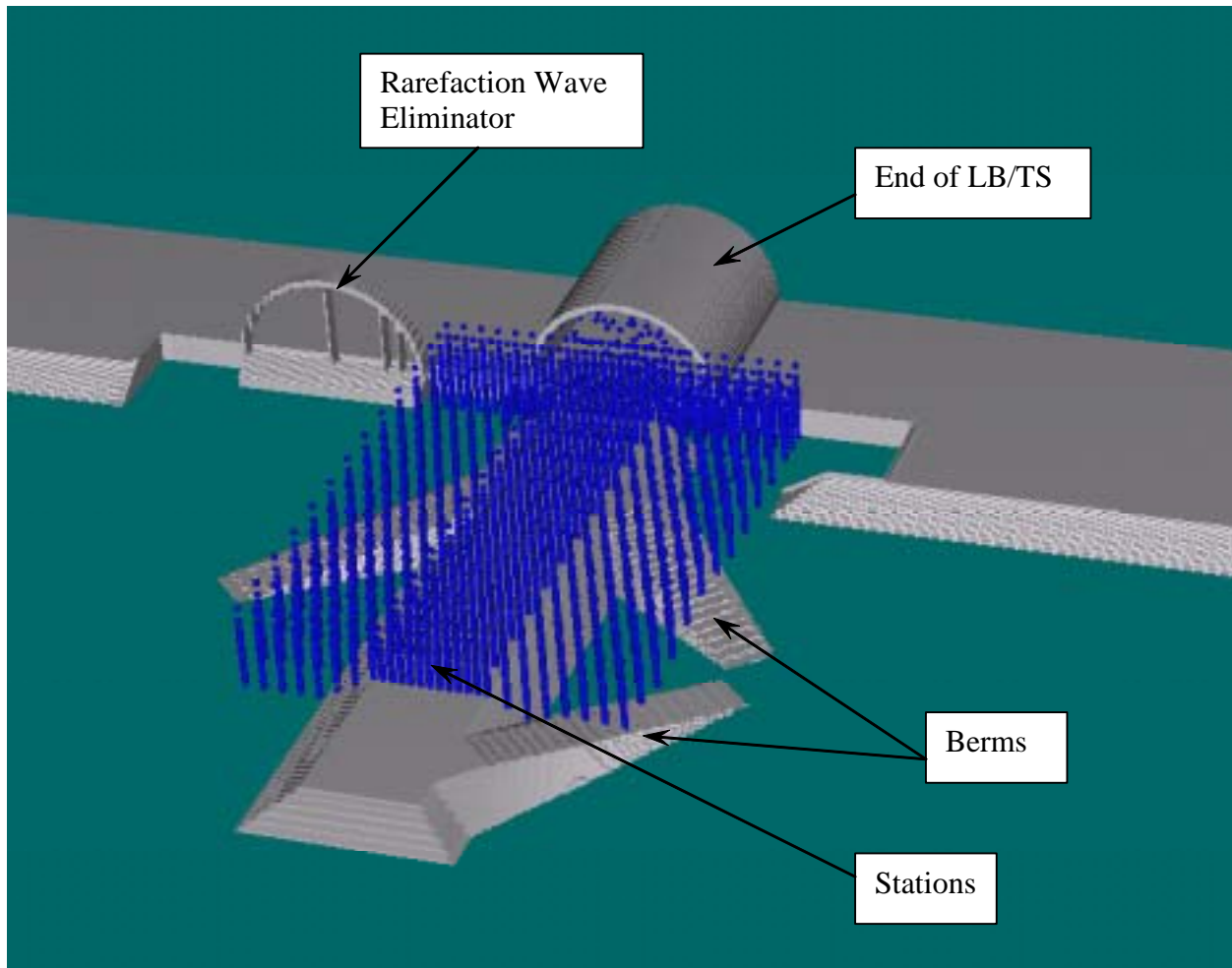


Figure 2 SHAMRC calculational model for the environment characterization simulations.

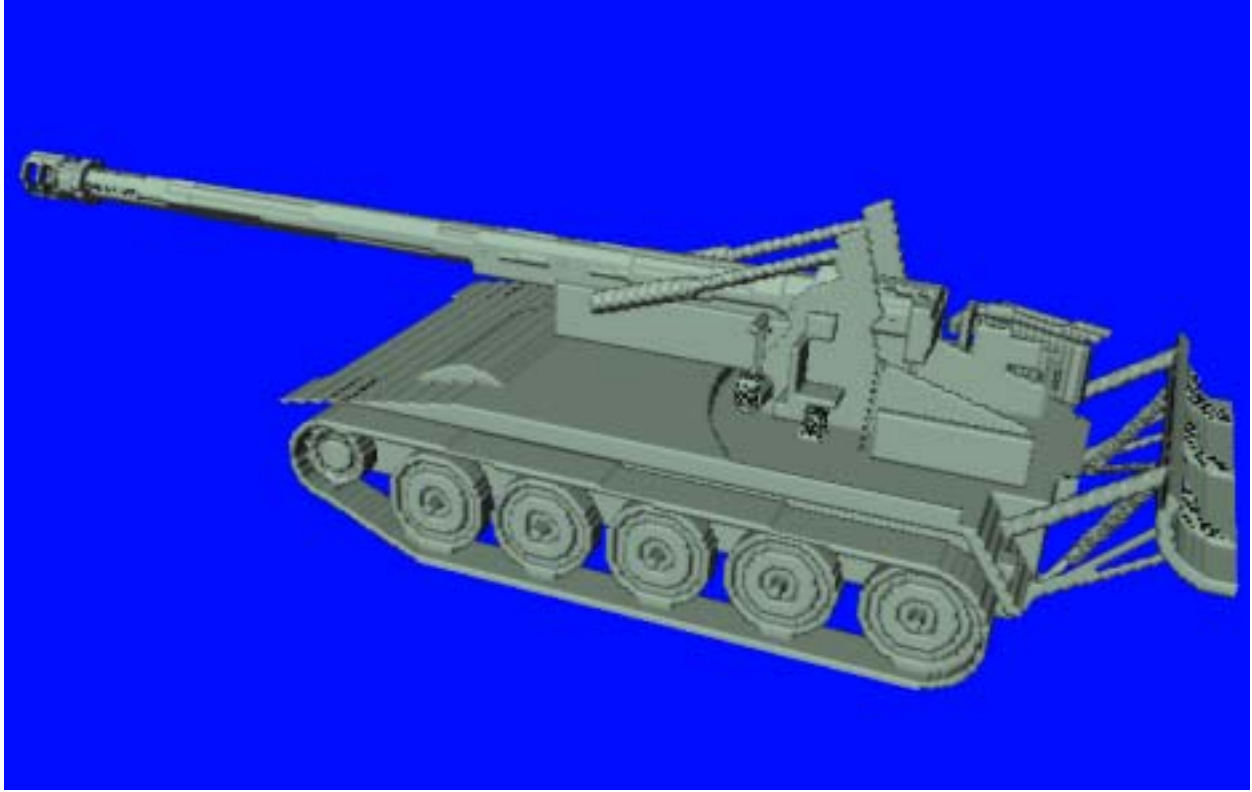


Figure 3 SHAMRC calculational model of M-110A2 for the vehicle loads simulation.

### Dust Injection Model

Two different dust injection models are available in SHAMRC to model the scouring of dust from the ground surface behind a blast wave. The first model, referred to as the  $\beta\rho U$  model, injects dust into zones adjacent to the ground surface proportional to the local fluid density and velocity. The second is used in conjunction with the K- $\epsilon$  turbulence model and injects dust proportional to the shear near the ground surface. Dust is treated as a fluid in the code. The mass is advected as any other material, but the dust does not contribute to the pressure of the zone.

For the two calculations reported here, the  $\beta\rho U$  model was used. This model was first used in a HULL calculation of an HE detonation over a dusty surface (Reference 3). The model is unchanged from its original implementation.

The equation used for the mass of injected dust is as follows.

$$\Delta m_i = A_i \beta \rho_i(\text{air}) |U_i| \Delta t$$

where

$\Delta m_i$  is the mass injected into cell  $i$  over time step  $\Delta t$   
 $A_i$  is the cross-sectional area of the cell



$\beta$  is the dust injection constant (0.6667)  
 $\rho_i$  is the air density  
 $U_i$  is the velocity of the cell (parallel to the surface)  
 $\Delta t$  is the time step

Two criteria must be met before dust mass is injected into a cell. First, the cell dust density must be below  $0.1 \text{ gm/cm}^3$ . Second, the dust is injected only when the kinetic energy (parallel to the surface) of the cell is above a threshold of  $750 \text{ gm/cm/sec}^2$ . Once these criteria are met, the fluid dust is injected into the cell with an initial velocity equal to  $1/10^{\text{th}}$  that of the velocity parallel to the surface and at an angle of 45 degrees in the direction of the flow. The injected dust is given an internal energy of  $1.443\text{e}9 \text{ ergs/gm}$ .

## HPC Resources Used

Both the environment and loads calculations were run with the parallel version of SHAMRC. The environment calculations were run on the Nirvana cluster at Los Alamos National Laboratories (LANL). The Nirvana cluster is a collection of 128-processor SGI Origin2000 boxes. The calculational grid contained approximately 48 million zones and required 70 hours of wall clock time on 128 processors on an SGI Origin2000.

The loads calculation was started on the LANL Nirvana cluster. At a problem time of 690 ms, the calculation was moved over to the SGI Origin3000 (ruby) at the US Army Engineer Research and Development Center (ERDC) and completed. On both systems, the calculation was run on 128 processors for the duration of the calculation. The calculation required 440 hours of wall clock time to complete. Based on an efficiency of 43 percent for an identical size problem, the equivalent runtime for the serial code would be approximately 18,920 hours or 2.2 years.

Each calculation required numerous dump files in order to produce a reasonable looking animation when the calculations were completed. The restart files for the environments calculation with dust were just over 1.3 Gbytes per file. Eighty restart files were saved for a total of 104 Gbytes of data. The 55 restart files for the loads calculation were just over 4.3 Gbytes per file for a total of 236 Gbytes of data.

## Data Comparisons

The results of the environment and loads calculations are in excellent agreement with the experimental data. Figure 4 is a sample overpressure waveform comparisons between the experimental data and the calculated data. The figure shows the SHAMRC environment calculation results from the calculations with and without dust overlaid on top of the experimental data trace. The waveform from the calculation without the dust (red dotted line) is in good agreement initially when the dust is not a factor. However, once the vortex arrives at the station, the waveform begins to deviate substantially from the experimental waveform. This is due to the presence of dust in the flow, which has been injected vertically by the vortex.

The calculation with dust (green dashed line) is in excellent agreement with the experiment out to times beyond 1 second. The presence of the dust in the vortex modifies the overpressure in this region and fills in the negative phase of the waveform. After the vortex passes, the wild

swings in the overpressure waveform without dust are reduced significantly and are in line with that observed experimentally. In addition, the overpressure impulse from the calculation with dust agrees extremely well with the experimental data impulse out to late times. Such agreement between experimental data and the dusty flow calculation provided confidence in the predictive capability of SHAMRC for vehicle loads calculations.

Waveform comparisons from the vehicle loads calculation are presented in

Figure 5 through Figure 7. Experimental gages were placed on the vehicle at three locations. They are on the upstream, downstream and bottom of the vehicle. Numerous stations were placed in the SHAMRC calculation on the surface of the vehicle model. These stations are indicated in the sub-figures as blue dots. The location of the station corresponding to the experimental gage is indicated as a red dot in the sub-figures. The experimental data traces are in black and the SHAMRC data traces are in blue.

Figure 5 is the comparison on the upstream side of the vehicle, above the tracks and not quite centered about the length of the vehicle. The calculated arrival time of the shock matches the experimental data exactly as does the initial peak and decay behind the peak. The experimental data shows the vortex arriving at about 440 ms. The calculation shows the vortex arriving 10 ms later. The overall waveform and the impulse are in very good agreement out to the time that the gage breaks at 590 ms.

Figure 6 compares the waveforms on the bottom of the vehicle. As with the upstream gage, the overall agreement between the calculation and the experimental data is quite good.

Figure 7 is a comparison on the downstream side of the vehicle. Again, the calculated arrival time is in excellent agreement with the experiment. Note that the pressure behind the initial shock from the experimental gage increases to a maximum of about 7 psi and then decays into a strong negative phase. The calculated pressure waveform exhibits the same behavior and matches the rise to the peak at 7 psi and the decay into the negative phase. The overpressure impulse is also in agreement.

Photographic data was also available from the tests. A comparison of a single frame from the experimental video and from the calculation at 690 ms is shown in Figure 8. The image from the calculation is a 3D rendering of a dust density isosurface at a value of  $1.e-5$  grams/cc. At this point in time, only the gun barrel and a small portion of the rear of the vehicle are visible. The agreement between the calculation and the test is remarkable. In fact, a time animation was produced from the calculation from essentially the same camera angle as that from the test. The authors worked closely with members of the ERDC graphics team to produce the animation. The calculation shows the same overall dusty flow conditions as that seen in test. That is, the relatively small dust injection into the flow until the arrival of the vortex, the height and angle of the dust in the flow, and the coverage of the vehicle of the dust in the flow.

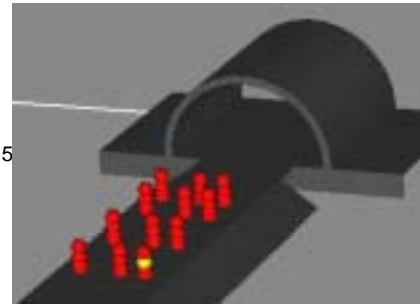
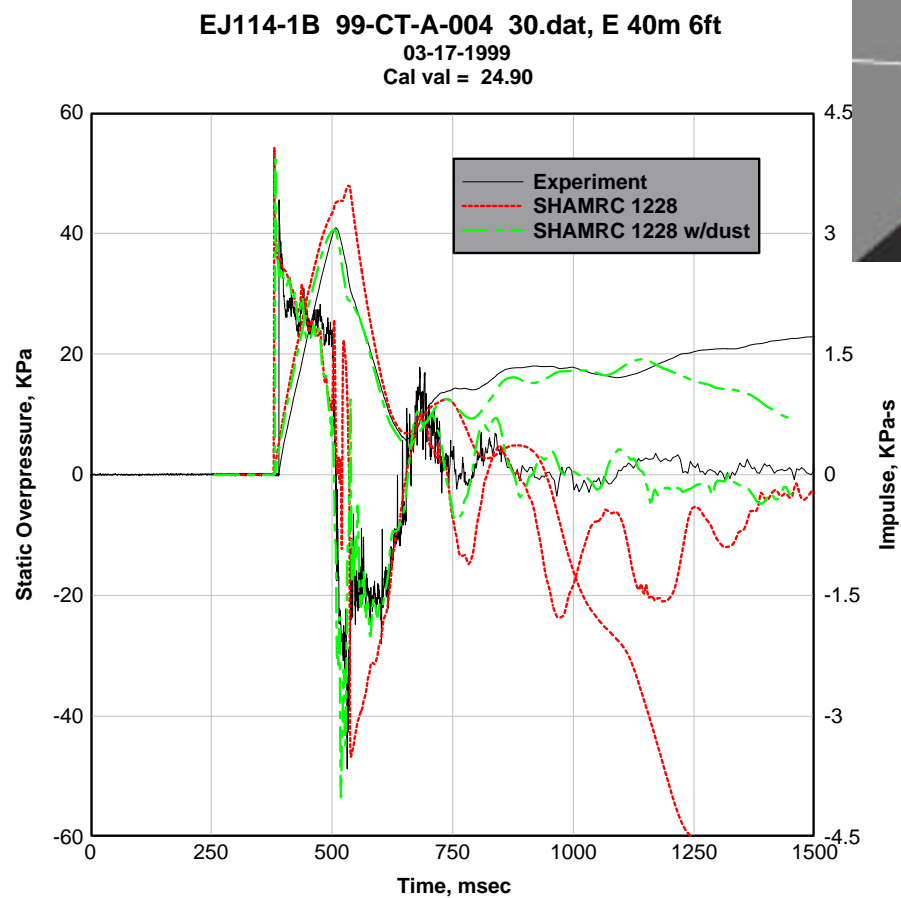


Figure 4 Waveform comparison between environment characterization test and SHAMRC. SHAMRC Calculations with (green, dashed) and without (red, dotted) dust. The insert shows the location of this station in yellow.

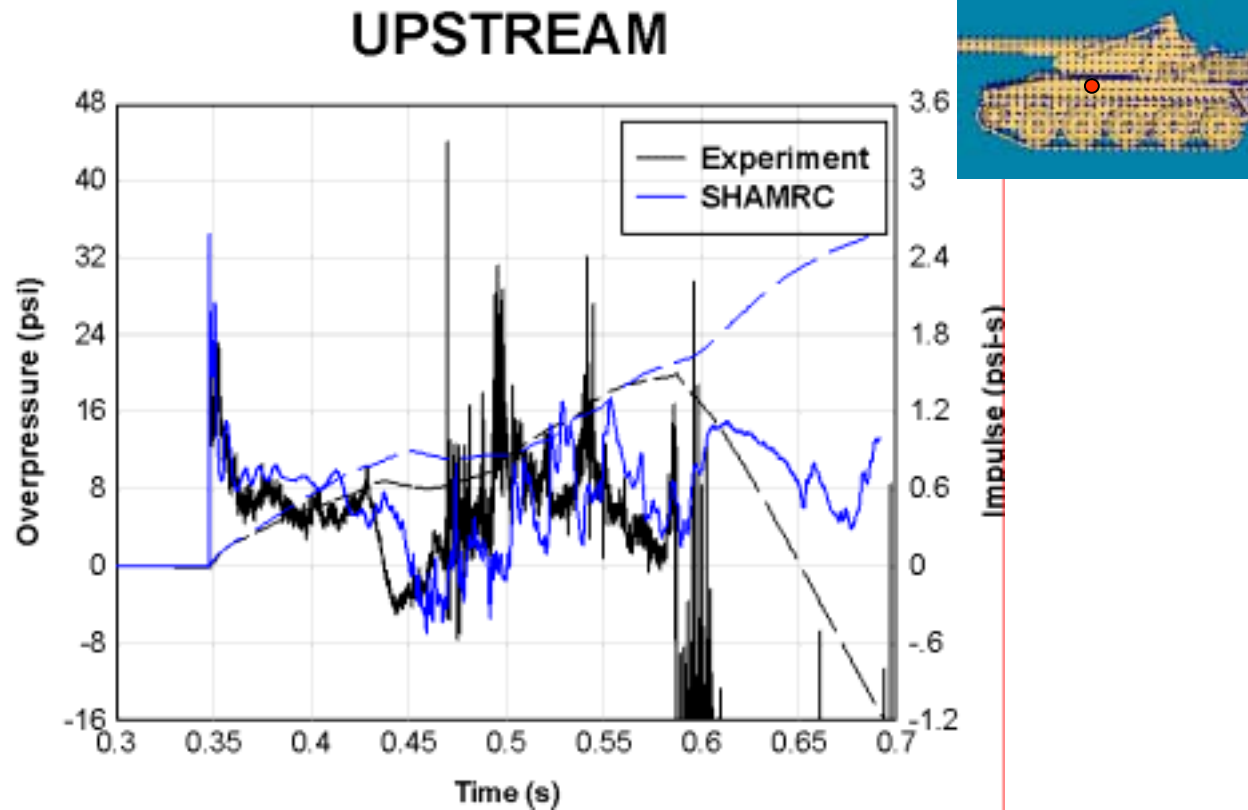


Figure 5 Overpressure waveform comparison between experimental gage recording (black) and SHAMRC calculation (blue) on upstream side of vehicle. The insert shows the stations on the vehicle surface (blue dots) and the location of this station in red.

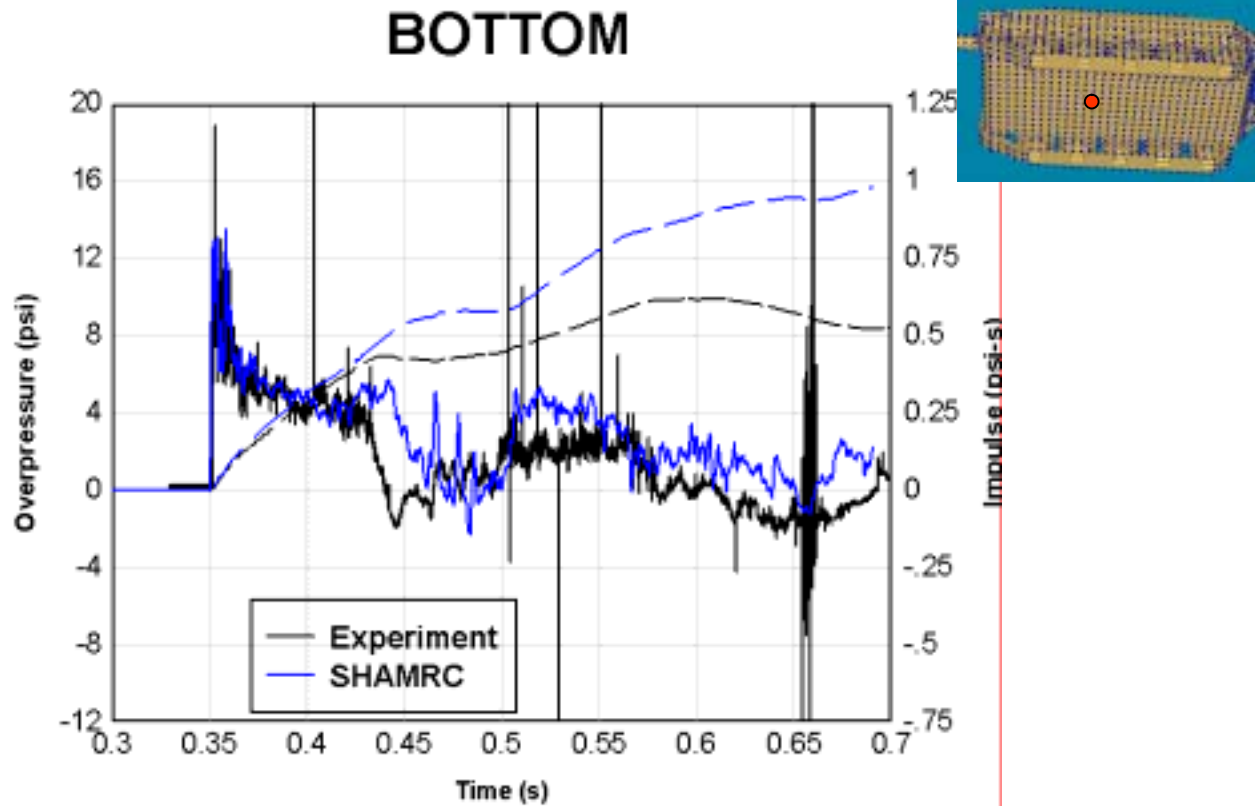


Figure 6 Overpressure waveform comparison between experimental gage recording (black) and SHAMRC calculation (blue) on bottom of vehicle. The insert shows the stations on the vehicle surface (blue dots) and the location of this station in red.

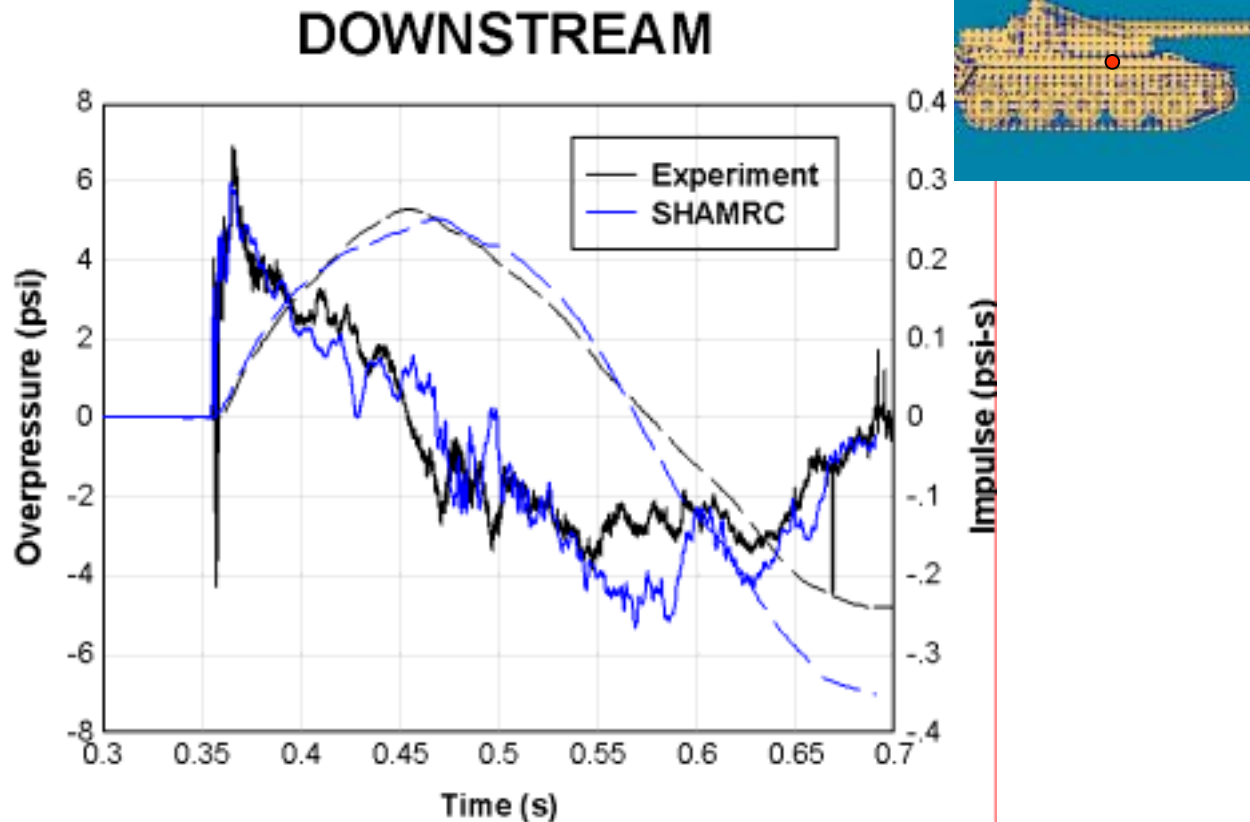


Figure 7 Overpressure waveform comparison between experimental gage recording (black) and SHAMRC calculation (blue) on downstream side of vehicle. The insert shows the stations on the vehicle surface (blue dots) and the location of this station in red.



Figure 8 Comparison of test video with SHAMRC image at 690 ms.

## Summary

HPC resources were successfully utilized to perform high-resolution SHAMRC calculations of the LB/TS exit jet environment and loads on a military vehicle. Comparisons of overpressure-time histories between the test and calculated data are in excellent agreement. The environment calculations showed the importance of modeling the entrainment of dust in the flow field in order to properly characterize the exit jet environment. Waveform comparisons on three sides of the vehicle were all in good agreement. Comparisons were also made between photographic data from the test and a 3D rendering of dust isosurfaces from the calculation and were in good agreement. An animation of the calculation was produced by the authors of this paper and members of the graphics support staff at ERDC. The resemblance between the test video and the calculation animation is striking.

The results of this effort would not have been possible without the use of HPC resources. This includes not only the computer time and data storage but also the use of the expertise of the graphics team at ERDC. By leveraging HPC resources, it was possible to complete highly reliable simulations of LB/TS tests in a timely manner. The results of the simulations allowed scientists to better understand the complex phenomena associated with non-ideal airblast and their interaction with vehicles.

## References

1. Crepeau, Joseph, Hikida, Shuichi, Needham, Charles E., "Second-order Hydrodynamic Automatic Mesh Refinement Code, Volume I: Methodology, 16 May 2001, pp58-62.
2. Newell, R.T., Crepeau, J.E., Needham, C.E., Ethridge, N.H., "LB/TS Tests of the Effects of Non-ideal Nuclear Air Blast on Military Vehicles", Applied Research Associates, Inc., ARA-LR-1.15-003, January 2001.
3. Joseph E. Crepeau and Charles E. Needham, "High Resolution Hydrodynamic Calculations of Free-Field Irregular Mach Reflection, Volume II: Dusty Surface," S-Cubed, S-82-5678, August 1982.